

# COMPARATIVE ANALYSIS OF COMPOUND PARABOLIC CONCENTRATOR RECEIVERS APPLIED TO SOLAR COOLING

I. Santos-González<sup>a\*</sup>, N. Ortega<sup>b</sup>, V.H. Gómez<sup>b</sup>, O. García-Valladares<sup>b</sup>, R. Best<sup>b</sup>

<sup>a</sup>Posgrado en Ingeniería (Energía), Universidad Nacional Autónoma de México, Privada Xochicalco s/n, Temixco, Morelos 62580, México.

<sup>b</sup>Centro de Investigación en Energía, Universidad Nacional Autónoma de México, Privada Xochicalco s/n, Temixco, Morelos 62580, México.

\*Corresponding Author: Iris Santos González, [irsag@cie.unam.mx](mailto:irsag@cie.unam.mx)

## Abstract

In the present work a comparative thermal study was realized. The comparison was limited to the receiver tubes of different materials for a specific compound parabolic concentrator (CPC), geometry. Inlet temperature range was selected from 30 to 70 °C and mass flow rate from 0.05 to 0.25 kg/s. The tests were performed with water as working fluid. Under these conditions, outlet temperature and irradiance were automatically recorded. Useful energy gain, absorbed solar radiation, overall heat loss coefficient and solar system efficiency were calculated.

The CPC studied has an aperture area of 1.33 m<sup>2</sup>, a real concentration ratio of 3.5 and an acceptance half-angle of 15°. The outside tube diameter remained constant an equal to 0.06m (2”).

The most suitable material was selected according to the experimental results. The specific CPC collector was designed to be applied as direct vapour generator of refrigerant. A theoretical model of a previously designed CPC (vapour generator) was coupled to an ammonia-water absorption refrigeration model in order to evaluate the performance of the complete refrigeration system. The absorption cooling system was designed for a 4.1kW cooling capacity. Low cost and easy manufacture make the developed CPC a good choice for low and medium temperature cooling applications in Mexico's marginal zones, where energy supply is excessively expensive or even does not exist.

## 1. Introduction

The CPCs are good choices for applications in direct evaporation, since these stationary collectors have a good quality rate between cost and performance at medium temperature levels [1]. The most important applications of this system are: heating water for domestic use, steam generation, cooking and solar cooling.

In a previous work [2], the theoretical analysis was emphasized into the evaporation process inside the CPC, through a detailed one-dimensional numerical simulation of the thermal and fluid-dynamic behaviour of two-phase flow.

For the receiver tube, in this work two materials were evaluated, carbon steel and aluminium (since the ammonia-water mixture is corrosive to copper), in order to choose the CPC with the better material receiver tube to be coupled to the absorption refrigeration system.

## 2. Numerical model description

The concentrator was designed using a one-dimensional model that solves in a segregated manner the fluid flow inside the receiver tube (in one or two phase flow), the heat conduction in

the receiver tube wall and the heat transfer in the solar concentrator. The initial conditions introduced in the numerical model were the geometry of the CPC, the boundary conditions (inlet temperature, pressure, mass flow rate, ambient temperature, wind speed and solar radiation), the place, date and time of the test. With this information the model can predict the increment of temperature between the inlet and outlet of the CPC, the thermal efficiency, the pressure drop as well as other variables, along the system.

To calculate the heat transfer coefficient in a single phase, the Gnielinski [3] correlation was used. The friction factor was evaluated using the expression proposed by Churchill [4], valid for all flow regimes.

### 3. CPC's geometry

The concentration (C) is one of the most important parameters for solar concentrator design. Intimately related to the concentration is the acceptance angle, that is the angular range over which radiation is accepted [5]. The concentration ratio is obtained from Eq. 1, which is defined as the ratio between the aperture area and the reception area.

$$C = \frac{A_c}{A_a} = \frac{1.33 \text{ m}^2}{0.378 \text{ m}^2} = 3.5 \quad (1)$$

Both receivers (carbon steel and aluminium) have a selective coating. Thermal conductivity was specified between 49.0 and 51.9 W/mK for the carbon steel case, and a constant value of 209 W/mK for the aluminium case.

Tables 1 and 2 show the designed CPC optical and geometrical characteristics, respectively.

Table 1. Optical properties of the designed CPC.

Component	$\alpha$ (dimensionless)	$\epsilon$ (dimensionless)	$\rho$ (dimensionless)	$\tau$ (dimensionless)
Receiver	0.91	0.38	0.09	–
Cover	0.03	–	0.05	0.94
Reflector	0.11	0.05	0.87	–

Table 2. Geometrical characteristics of the designed CPC.

$\theta_c$ (degrees)	C (dimensionless)	$A_c$ (m <sup>2</sup> )	$D_i$ (mm)	H (m)	W (m)	L (m)
15	3.5x	1.33	52.5	0.81	0.66	2.00

### 4. Coupling between the CPC and a one-stage absorption refrigeration system model

Fig. 1 shows the arrangement of the CPC coupled to the cooling system of a continuous absorption stage. The capacity of the proposed absorption cooling is 4.1 kW with a COP of 0.45 [6].

Numerical analysis was carried out for the previously designed CPC, coupled to the single stage ammonia-water absorption solar refrigerator that consists of a generator (CPC), a rectifier, a condenser, an evaporator, an absorber, an economizer, a pre-cooler, two valves and a solution pump. The energy balance analysis over each component of the system was coupled with the CPC model in order to evaluate the performance of the complete ammonia-water absorption

refrigeration system in order to calculate the coefficient of performance (COP), the flow ratio, the solar fraction, and the solar and overall efficiency. The theoretical results were previously reported [6].

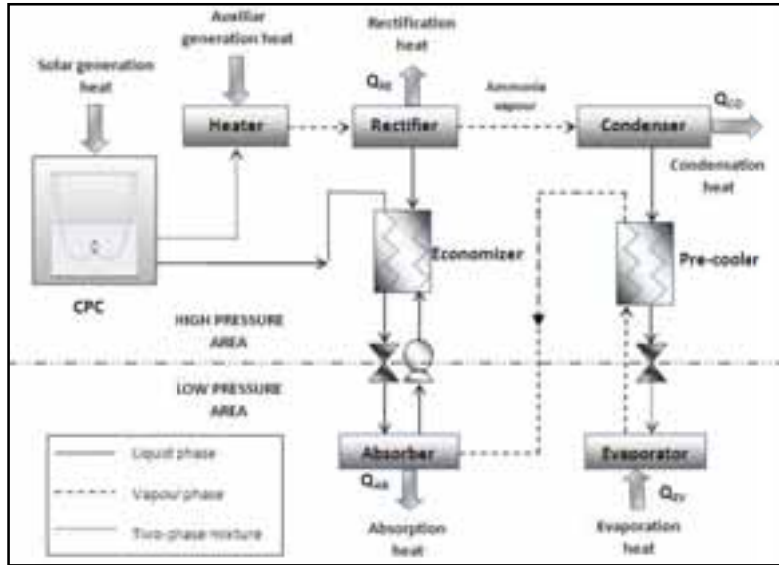


Fig. 1. The CPC coupled to a continuous absorption solar refrigerator system.

## 5. Experimental set up

An experimental apparatus was designed and built. A proper instrumentation to control and register the different variables of the system together with a program to save the experimental data was developed.

The experimental unit consists in following elements: The CPC, two storage tanks, a re-circulating pump, a support structure with variable angles of  $0^\circ$ ,  $10^\circ$ ,  $21^\circ$  and  $30^\circ$ , a Coriolis mass flow meter, a differential pressure meter, a pyranometer, two temperature sensors, and twenty eight J-type thermocouple sensors to measure along the receiver tube. The experimental system is shown in Fig. 2.

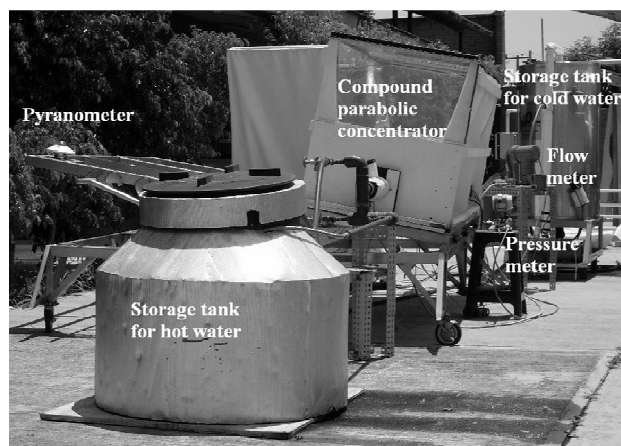


Fig. 2. Experimental set up.

### 5.1 Experimental tests

The experimental tests were performed with water as working fluid, in a range of temperature from  $30^\circ\text{C}$  to  $70^\circ\text{C}$ , mass flow rates from  $0.05\text{ kg/s}$  to  $0.25\text{ kg/s}$ , and CPC slopes of  $0^\circ$  and  $10^\circ$ , the adjustment corresponding to March and May months.

The experimental sequence took place as follows:

- CPC mass flow rate and inlet temperature were set and maintained constant.
- The CPC inlet and outlet temperatures and pressure were registered.
- The water coming from the CPC was stored in a second tank.
- The experimental test was finished.
- The water in the second tank was returned to the first tank to fix a new temperature and a new mass flow rate to repeat the process.
- All the variables in the system were registered every 10 seconds.

## 6. Comparative analysis of the receivers

Experimental and numerical concentrator outlet temperatures, for the aluminium and carbon steel receiver tubes, at a constant mass flow rate of 0.2 kg/s, are shown in Table 3. The experimental values are reported with its standard deviation.

Table 3. Comparison of numerical and experimental outlet temperature for aluminium and carbon steel receivers at a mass flow rate of 0.2 kg/s.

$(T_{in}-T_{amb})/I$ (°C m <sup>2</sup> /W)	Carbon steel (°C)		Aluminium (°C)	
	Experimental	Numerical	Experimental	Numerical
0.0010	35.85±0.01	35.68	32.93±0.08	33.39
0.0051	–	–	41.86±0.05	41.95
0.0066	41.75±0.05	41.72	–	–
0.0067	43.00±0.01	43.00	–	–
0.0069	–	–	41.92±0.04	42.05
0.0071	–	–	42.89±0.06	42.90
0.0145	–	–	50.87±0.04	50.88
0.0147	–	–	50.93±0.05	50.88
0.0154	51.02±0.02	51.00	–	–
0.0156	–	–	50.63±0.05	50.48
0.0219	60.91±0.03	60.98	–	–
0.0242	60.39±0.04	60.35	–	–
0.0252	–	–	59.03±0.11	59.01
0.0275	–	–	59.33±0.07	59.06
0.0340	–	–	68.38±0.06	68.44
0.0357	69.59±0.02	69.48	–	–
0.0370	69.85±0.03	69.79	–	–

As is shown in Table 3, the average difference between experimental and numerical results is ±0.10 °C for the carbon steel receiver, and ±0.14 °C for the aluminium receiver.

Fig. 3 shows the numerical and experimental increment of temperature for the carbon steel and aluminium at mass flow rate of 0.25 kg/s. The average radiation for the carbon steel receiver

tests was  $1044 \text{ W/m}^2$ , and  $872 \text{ W/m}^2$  for the aluminium receiver tests. The difference between the experimental and numerical temperature increment was  $\pm 0.06 \text{ }^\circ\text{C}$  for the carbon steel receiver, and  $\pm 0.05 \text{ }^\circ\text{C}$  for the aluminium receiver. Errors bars represent the uncertainty obtained in the experimental measurement.

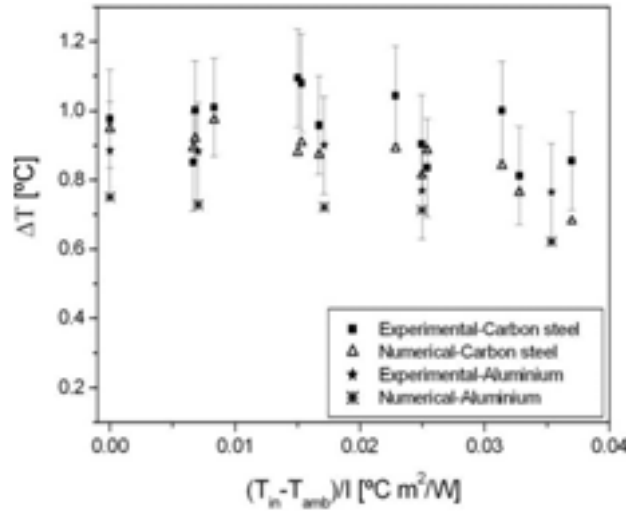


Fig. 3. Comparison of increment of temperature for the experimental and numerical results with a mass flow rate of 0.25 kg/s.

Fig. 4 shows that in spite of the received energy variation, the carbon steel receiver tube have a good surface temperature distribution, similar to the aluminium receiver.

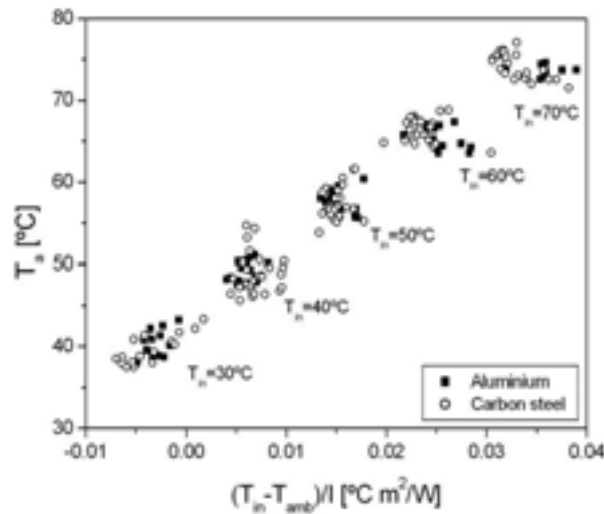


Fig. 4. Average temperature distribution in the carbon steel and aluminium receiver tubes.

In a typical efficiency curve, the ratio between the intercept and the slope is a measure of the energy gain with respect to the energy loss (Eq. 2).

$$\frac{b}{m} = -\frac{1}{CI} \frac{S}{U_L} \quad \rightarrow \quad \frac{S}{U_L} = -CI \frac{b}{m} \quad (2)$$

The following results were obtained from the experimental data, with a solar irradiance constant of  $1000 \text{ W/m}^2$ , and mass flow rate of  $0.05 \text{ kg/s}$  and  $0.25 \text{ kg/s}$ :  $(S/U_L)_{0.05\text{-carbon-steel}}=439 \text{ K}$ ,  $(S/U_L)_{0.05\text{-Aluminium}}=367 \text{ K}$ ,  $(S/U_L)_{0.25\text{-carbon-steel}}=1039 \text{ K}$  y  $(S/U_L)_{0.25\text{-Aluminium}}=650 \text{ K}$ . The same procedure was performed for the numerical results:  $(S/U_L)_{0.05\text{-carbon steel}}=936 \text{ K}$ ,  $(S/U_L)_{0.05\text{-}}$

Aluminum=798 K,  $(S/U_L)_{0.25}$ -carbon steel=704 K y  $(S/U_L)_{0.25}$ -Aluminum=585 K. In general, the carbon steel receivers produced better experimental and numerical results, than the aluminium receptor.

Figs. 5 and 6 show the efficiency calculated with the experimental data and the numerical results for the carbon steel receiver and the aluminium receiver for a mass flow rate of 0.25 kg/s.

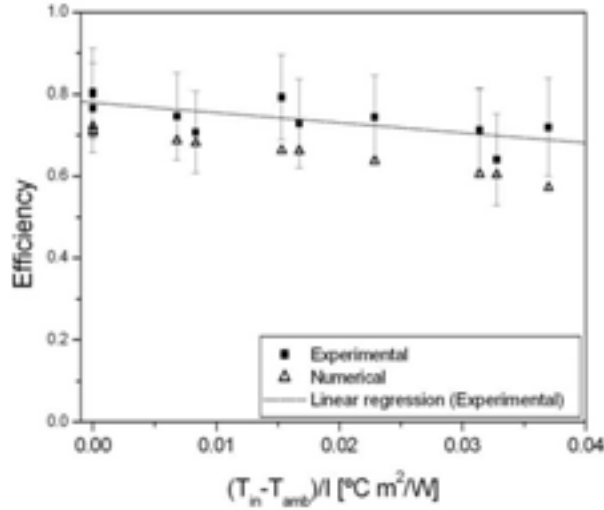


Fig. 5. Efficiency obtained with experimental data and numerical results for the carbon steel receiver, with a mass flow rate of 0.25 kg/s.

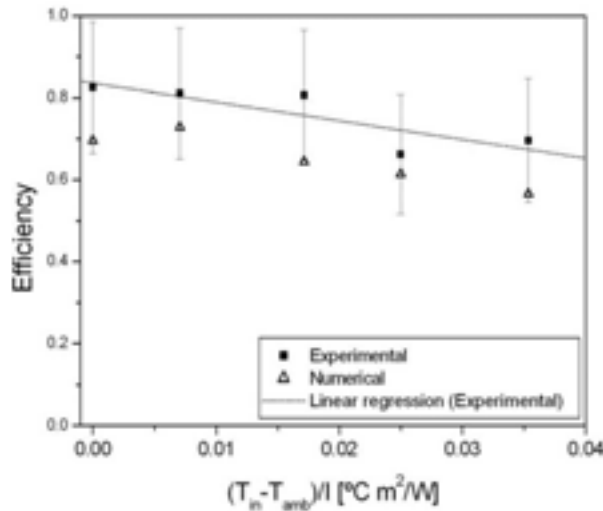


Fig. 6. Efficiency obtained with experimental data and numerical results for the aluminium receiver, with a mass flow rate of 0.25 kg/s.

From Fig. 5 it is seen that the efficiency curve for the experimental data of the carbon steel receiver, with a mass flow rate of 0.25 kg/s, is (Eq. 3):

$$\eta = 0.781 - 2.496 \frac{T_{in} - T_{amb}}{I} \quad (3)$$

And from Fig. 6, the efficiency curve for the experimental data of the aluminium receiver, with a mass flow rate of 0.25 kg/s, is (Eq. 4):

$$\eta = 0.836 - 4.499 \frac{T_{in} - T_{amb}}{I} \quad (4)$$

The comparison between the two receiver tube materials was carried out. In stationary state, the receiver tube material does not significantly influence the outlet temperature, and has some impact in the efficiency, as shown in Table 4; however, material selection must be done carefully for each specific application, due to corrosion caused by ammonia-water mixture as in the study case.

Table 4. Experimental results to compare the two materials.

Material	I (W/m <sup>2</sup> )	$\Delta T$ (°C)	$\eta$ (dimensionless)	$\dot{m}$ (kg/s)
Carbon steel	905.03	1.34	0.70	0.15
Aluminium	904.01	1.44	0.75	0.15

Finally, for the refrigeration study case, with a 4.1 kW cooling capacity and the following assumptions: an inlet temperature for the CPC as ammonia generator of 81.65 °C, a mass flow rate of 0.25kg/s, an ambient temperature of 33 °C and a irradiance of 950 W/m<sup>2</sup> (the averages values obtained during the test days), from the Eqs. 3 and 4 the solar efficiency of the CPC will be 0.653 for the carbon steel receiver and 0.606 for the aluminium receiver, acceptable values for these kinds of cheap and easy of manufacture systems.

## 7. Conclusions

The system proved thermal stability and functionality, reaching steady state after two minutes of operation.

Both receiver tubes have similar behaviour in terms of outlet temperature and efficiency, although carbon steel receiver has a slightly better performance; however the aluminium is recommended for its lightness and also because it is compatible with the ammonia-water mixture, using in absorption refrigeration systems. For the refrigeration study case, a receiver of carbon steel will be better than one of aluminium, since its solar efficiency is 5% higher.

Finally, the average deviation in the efficiency (at the entire operation conditions) between the numerical model and the experimental results was  $\pm 13.94\%$  for the carbon steel receiver, and  $\pm 14.22\%$  for the aluminium receiver; while the average outlet temperature deviation was  $\pm 0.37^\circ\text{C}$  for the carbon steel receiver, and  $\pm 0.47^\circ\text{C}$  for the aluminium receiver.

## 8. Acknowledges

This document has been produced with the financial assistance of the European Union and Mexico. The contents of this document are the sole responsibility of Centro de Investigación en Energía de la Universidad Nacional Autónoma de México and can under no circumstance be regarded as reflecting the position of the European Union and Mexico.

The first author would like to thanks CONACYT for the received scholarship number 231315.

## 9. Nomenclature

A	Heat transfer area [m <sup>2</sup> ]
b	Intercept
C	Solar concentration [dimensionless]
D	Diameter [m]
H	Height [m]

I	Solar irradiance [W/m <sup>2</sup> ]
L	Length [m]
m	Slope [W/(m <sup>2</sup> K)]
$\dot{m}$	Mass flow rate [kg/s]
Q	Heat flow [W]
S	Solar absorber energy per unit area [W/m <sup>2</sup> ]
T	Temperature [°C]
U <sub>L</sub>	Overall heat loss coefficient [W/(m <sup>2</sup> K)]
W	Width [m]

### Greek letters

$\alpha$	Absorptance [dimensionless]
$\varepsilon$	Emittance [dimensionless]
$\eta$	Efficiency [dimensionless]
$\theta_c$	Acceptance half-angle [degrees]
$\rho$	Reflectance [dimensionless]
$\tau$	Transmittance [dimensionless]
$\Delta T$	Temperature difference [°C]

### Subscripts

a	Receiver
AB	Absorber
amb	Ambient
c	Cover
CO	Condenser
EV	Evaporator
i	Inside
in	Inlet
out	Outlet
RE	Rectifier

## 10. References

- [1] Collares-Pereira M. (1995). CPC type collectors and their potential for solar energy cooling applications, Proceedings of the 2nd. Munich Discussion Meeting "Solar Assisted Cooling with Sorption Systems", Munchen, paper 5.
- [2] Ortega N., García-Valladares O., Best R., Gómez V.H. (2008). Two-phase flow modelling of a solar concentrator applied as ammonia vapour generator in an absorption refrigerator, *Renewable Energy*, 33, 9, pp. 2064-2076.
- [3] Gnielinski V. (1976). New equations for heat and mass transfer in turbulent pipe and channel flow, *International Chemical Engineering*, 16, pp. 359-368.
- [4] Churchill S.W. (1977). Frictional equations spans all fluid flow regimes, *Chemical Engineering*, 84, pp. 91-92.
- [5] Rabl A. (1976). Comparison of solar concentrators, *Solar Energy*, 18, pp. 93-111.
- [6] Ortega N., García-Valladares O., Best R., Gómez V.H. (2007). Heat transfer in components and systems for sustainable energy technologies, Proceedings of the Heat Transfer in Components and Systems for Sustainable Energy Technologies: Heat SET 2007, Chambéry, France.